Network Equipment and Their Procurement Strategy for High Capacity Elastic Optical Networks

Abhijit Mitra, David Ives, Andrew Lord, Seb Savory, Subrat Kar, and Paul Wright

***Abstract*—In elastic optical networks, the success of providing high network capacity depends on the optical signal-to-noise ratio (OSNR) values of network lightpaths. As each lightpath's OSNR value defines the modulation format and capacity it can support, having high OSNR lightpaths is always beneficial. Hence, with a given set of modulation formats, service providers need to optimize their optical infrastructure, including in-line amplifiers and reconfigurable optical add–drop multiplexers (ROADMs), given the size and topology of their core networks. This also will have a direct impact on vendors who need strong insight into the requirements of service providers and their networks in terms of equipment and new technology. Therefore, in this paper a comprehensive model based on the local optimization which leads to a global network optimization (LOGON) strategy of the Gaussian noise (GN) model has been proposed, which helps in estimating the lightpath OSNR and clearly quantifies the noise contributions from in-line amplifiers and post-amplification at the ROADMs. The model introduces closed-form expressions to calculate nonlinear impairment (NLI) contributions for various span lengths while using either erbium-doped fiber amplifiers (EDFAs) or H-Raman amplifiers, which helps in optimizing the signal launch power to achieve maximum link OSNR. In addition to this, an offline strategy has been proposed that can help service providers to optimize their procurement of network equipment upfront and give insight into how much of the capacity bottleneck is alleviated in their networks if they do this. To demonstrate all of the above, the UK, Pan-European, and US Core networks have been considered, which illustrate differences in link lengths and reduced node density. It is seen that improving the OSNR conditions at the ROADM increases the network capacity when noise from in-line amplifiers is significantly reduced. Among the three networks, we found that the UK network responded the most to improved OSNR conditions at the ROADM nodes due to small link lengths and less line noise. Among the amplifiers, we found that improving ROADMs while having H-Raman in the links resulted in a maximum capacity increase. For the UK network at FG = 12.5 GHz, the capacity increases by 6650 Gbps, while for the larger Pan-European and US networks, the capacity increase reduces to 4550 and 1600 Gbps due to increased link lengths and line noise. Further, following the offline strategy, we are able to accommodate 1737, 1481, and 615 100G demands using H-Raman for the UK, Pan-EU, and US networks at FG = 12.5 GHz until 10% blocking is reached. Thereby, H-Raman provides 7.5%, 35.8%, and 94.9% extra capacity, respectively, for the UK, Pan-EU, and US. Finally, using H-Raman, all lightpaths in the UK network operate at PM-64QAM with maximum capacity at the end of the procedure.**

***Index Terms*—CapEx; Network equipment upgrade; Network management; OSNR estimation with nonlinear impairments.**

I. Introduction

Elastic optical networks (EONs) aim to improve network capacity by using flexible spectrum channels and higher-order modulation formats [1,2]. However, depending upon link lengths and the geographical area of a network, the choice of in-line amplifiers and reconfigurable optical add–drop multiplexers (ROADMs) is crucial to achieve these aimed-for high network capacities and capitalize on the wide heterogeneity of available modulation formats in EONs. In addition to this, it is important for service providers to strategically make use of superior optical amplifiers and ROADMs in order to justify the inevitable increase in capital expenditure (CapEx) through gains in potential network capacity.

Earlier research strides were taken in network planning and CapEx [3,4], which sought to reduce the expenditure of overall IP/MPLS layer equipment and take advantage of the flexibility of EONs. However, both assumed the performance of the lightpaths rather than including it in the model. To carry these benefits further, it is important to model the physical layer transmission parameters to reliably predict the state of network lightpaths. The model should account for the nonlinear impairments (NLIs) present in the optical links and also account for noise contributions from in-line amplifiers and ROADMs. Recently, significant work has been done in [5,6] to include NLI in the Gaussian noise (GN) model. The result of this leads to network optimization based upon local optimization which leads to a global network optimization (LOGON) strategy [5]. However, to study noise contributions from in-line amplifiers and ROADM nodes in a network context,

Manuscript received December 2, 2015; revised June 10, 2016; accepted June 10, 2016; published July 1, 2016 (Doc. ID 254809).

A. Mitra is a BT research fellow at the Indian Institute of Technology Delhi, New Delhi 110016, India (e-mail: abhijit.mitra@bt.com).

D. Ives and S. Savory are with the Electrical Engineering Division, Department of Engineering, University of Cambridge, Cambridge CB30FA, UK.

A. Lord and P. Wright are with the British Telecommunication Core Networks Research at Adastral Park, Martlesham, Ipswich IP53RE, UK.

S. Kar is a professor in the Electrical Engineering Department and is associated with the Bharti School of Telecom Technology and Management, Indian Institute of Technology Delhi, New Delhi 110016, India.

http://dx.doi.org/10.1364/JOCN.8.00A201

we further simplify this model so that the benefit of using better equipment in terms of network capacity can be predicted.

In this paper, we simplify the GN model to derive closed-form expressions to predict normalized nonlinear coefficients, used to estimate the NLI for various span lengths. The closed-form expressions are calculated at frequency granularity (FG) of 50 and 12.5 GHz for erbium-doped fiber amplifiers (EDFAs) and hybrid-Raman (H-Raman) amplifiers. Further, a closed-form expression for the effective noise figure for H-Raman has been derived to account for amplified spontaneous emission (ASE) noise. Using these expressions, we further derive expressions for the optimum signal launch power to provide the maximum link optical signal-to-noise ratio (OSNR), taking into account the number of spans, span length, ASE, and NLI contributions for that link. All the above expressions are necessary to quantify the benefit to network capacity of using EDFAs, H-Raman amplifiers, and improved ROADMs. Using this model, we show that the benefits from improved OSNR at ROADMs are achieved for networks with high node density, and these benefits are further enhanced when the dominant noise from the in-line amplifiers is significantly reduced by either reducing the span length or using superior amplifiers such as H-Raman. Finally, using the NLI model, we also demonstrate an offline network planning strategy for the UK, Pan-European (EU), and US network, assisting service providers with optimal amplifier procurement and illustrating directly the benefits of procuring additional equipment upfront. In this process, we use the capacity constraint (CC) factor [7] to understand the state of network lightpaths from which we deduce whether an operator should use CapEx to acquire better quality in-line amplifiers or better ROADMs.

II. Network NLI Transmission Model

In Fig. 1, a small network topology is shown to demonstrate the working of the noise model. Starting with a higher signal power P_r, the signals are attenuated by the attenuators (gray) down to an optimum signal power, P^i_{opt}, as they enter an ith fiber link.

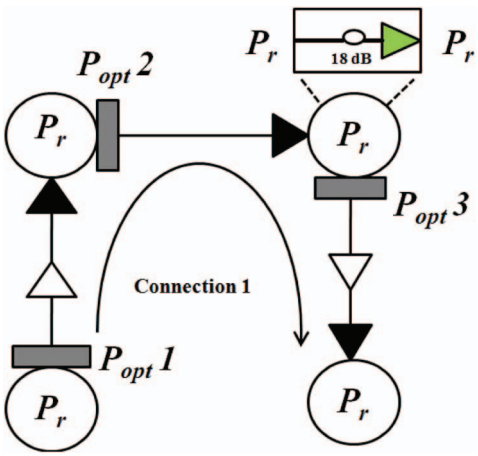

Fig. 1. Network model.

Throughout the link, this optimum power profile is maintained to reduce the effect of NLI. Each intermediate amplifier compensates for the previous span loss, apart from the last amplifier, which increases the signal power at the node back to P_r. The ROADM loss is assumed to be 18 dB. Here P_r is the maximum optimum launch power value among all the fiber links in the network [7] with a maximum span length (MaxSpan) of 120 km. This distance has been fixed, assuming that optical amplifiers can provide a gain of up to 30 dB [8]. The NLI noise power of an optical link with NS spans can be calculated from Eq. (1):

$$\eta_{\text{NLI}} = \left(\frac{P_r}{P^{\text{new}}_{opt}}\right) N_s (P^{\text{new}}_{\text{opt}})^3 X_m(L), \tag{1}$$

where $X_m(L)$ is the normalized nonlinear coefficient calculated for each span of length of L km and reference bandwidth: B_{ref} of 12.5 GHz [7]. The $X_m(L)$ coefficients are calculated from the power spectral density equations of the GN model [7] for the EDFA and backward-pumped H-Raman cases and correspond to the maximum NLI on the worst-case central channel for fully loaded links. $P^{\text{new}}_{\text{opt}}$ is the optimum signal launch power in an optical fiber link.

From [7], it is shown that the OSNR of a lightpath is calculated from Eqs. (2) and (3):

$$\text{OSNR}^{-1}_{\text{path}} = \sum_{i=1}^{N_L} \left(\frac{P_r}{\text{ASE}_{Li} + \eta^i_{\text{NLI}}}\right)^{-1} + \left(\frac{P_r}{\text{ASE}_R}\right)^{-1} N_R, \tag{2}$$

$$\text{OSNR}^{-1}_{\text{path}} = \left(\sum_{i=1}^{N_L} \frac{1}{\text{OSNR}_i}\right) + \left(\frac{1}{\text{OSNR}_R}\right) N_R. \tag{3}$$

OSNR_i is the ith link OSNR, which represents the contribution from line amplifiers in a link, and OSNR_R is the OSNR contribution from the ROADMs. The ASE_{Li} terms depend upon the noise performance of amplifiers, which are placed symmetrically in the link and the ASE_R term produced by post-amplifiers (green) in ROADMs compensating for 18 dB loss. Both ASE_{Li} and ASE_R are ASE noise powers. In the consecutive subsections, expressions for calculating total $Xm(L)$ and $P^{\text{new}}_{\text{opt}}$ are derived for the Fig. 1 scenario. NL is the link number of the last traversed link, and NR is the total number of traversed intermediate ROADMs. Similar expressions have also been recently suggested in [9,10].

A. Only EDFA System

The total ASE noise introduced from the EDFAs of an optical link is given by Eq. (4) [7]:

$$\text{ASE}_0 = \left[\left(\frac{P_r}{P^{\text{new}}_{\text{opt}}}\right) N_s \text{ASE}_1 + 2n_{\text{sp}} h\nu \left(\frac{P_r}{P^{\text{new}}_{\text{opt}}} - 1\right) B_{\text{ref}}\right], \tag{4}$$

$$\text{ASE}_1 = 2n_{\text{sp}} h\nu (g-1) B_{\text{ref}}. \tag{5}$$

TABLE I
COEFFICIENT VALUES FOR $X_m^{\mathrm{ED}}(L)$ PREDICTIONS

FG	a	b	c
50 GHz	0.0004212	−0.09673	1.1893
12.5 GHz	0.0005680	−0.09892	1.1654

In Eq. (5), ASE_1 is the ASE noise from intermediate amplifiers calculated over B_{ref} of 12.5 GHz, n_{sp} is the spontaneous emission factor, h is Planck's constant, v is the channel carrier optical frequency, and g the linear amplifier gain. Using the GN model, $X_m(L)$ was calculated [7] over the entire C band for the center channel, which accounts for the worst-case NLI [11] for both FG = 12.5 GHz and FG = 50 GHz with 133 and 100 channels, respectively. Using Eq. (6) and Table I coefficient values, we can predict $X_m(L)$ values for the EDFA case denoted by $X_m^{\mathrm{ED}}(L)$:

$$X_m^{\mathrm{ED}}(L) = a(1 - \exp(b \times L))^c. \tag{6}$$

The OSNR of an optical link can be approximated by Eq. (7):

$$\mathrm{OSNR} = \frac{P_r}{\mathrm{ASE}_0 + \eta_{\mathrm{NLI}}}. \tag{7}$$

Substituting Eqs. (1) and (4) into Eq. (7), and differentiating for $P_{\mathrm{opt}}^{\mathrm{new}}$, in order to maximize OSNR in an optical link, we get the new optimum signal launch power for that link:

$$P_{\mathrm{opt}}^{\mathrm{new}} = \left(\frac{n_{\mathrm{sp}} h v((N_s 10^{\alpha L/10}) - N_s + 1) B_{\mathrm{ref}} 1000}{N_s X_m^{\mathrm{ED}}(L)}\right)^{1/3}. \tag{8}$$

Using Eq. (8), with given network specifications, we can simply generate a list of new optimum powers for each fiber link in a network. For the EDFA case, P_r is 1.6 mW at MaxSpan = 120 km [7] and α is the signal power loss per km.

B. $X_m(L)$ Expressions for a Backward-Pumped H-Raman System

In [6,11] the PSD of the nonlinear interference for a single-span NLI, $G_{\mathrm{NLI,SS}}$ is given by

$$G_{\mathrm{NLI,ss}} = \frac{16}{27}\gamma^2 L_{\mathrm{eff}}^2 \int_{-\infty}^{\infty}\int_{-\infty}^{\infty} G(f_1)G(f_2)G(f_1+f_2-f) \times \rho(f_1,f_2,f_3)\mathrm{d}f_1\mathrm{d}f_2. \tag{9}$$

From derivation in Appendix A, we find the $X_m(L)$ expression over B_{ref} of 12.5 GHz for H-Raman denoted by $X_m^{\mathrm{H\text{-}Ram}}(L)$ given in Eq. (10):

$$X_m^{\mathrm{H\text{-}Ram}}(L) = \frac{B_{\mathrm{ref}}}{R}\frac{16}{27}\gamma^2 \int_{-\infty}^{\infty}\int_{-\infty}^{\infty}\int_{-\infty}^{\infty}\Big[g(f_1)g(f_2)g(f_1+f_2-f) \times H(f)L_{\mathrm{eff}}^2\rho(f_1,f_2,f)\mathrm{d}f_1\mathrm{d}f_2\mathrm{d}f\Big]. \tag{10}$$

The integration of Eq. (10) is done by the Monte Carlo simulation method, which gives some degree of uncertainty over the calculated values of $X_m^{\mathrm{H\text{-}Ram}}(L)$ for both FG = 50 and 12.5 GHz. For solving the integral, we use the fiber parameters for a standard single-mode fiber (SSMF) with pump loss $\alpha_p = \alpha = 0.25$ dB/km (0.057565 km^{-1}), dispersion coefficient of the fiber $\beta_2 = 16.7$ ps/(nm · km), fiber nonlinearity coefficient $\gamma = 1.3$ $(\mathrm{W \cdot km})^{-1}$, baud rate $R = 27.75$ GBd, and on–off gain $G_{\mathrm{oo}} = 10$ dB. The GN model has been used in its incoherent form. The calculated mean $X_m^{\mathrm{H\text{-}Ram}}(L)$ values are given in Table II, along with the standard deviation for each value. Using the weighted least-squares regression method and with standard deviation as weights in the MATLAB curve fitting tool, we have found generalized functions for both FG = 50 GHz and FG = 12.5 GHz with a precision of 10^{-7}. Equation (11) is the generalized form with its coefficient values given in Table III for each FG:

$$X_m^{\mathrm{H\text{-}Ram}}(L) = ae^{(bL)} + ce^{(dL)}. \tag{11}$$

In Fig. 2, the behavior of $X_m^{\mathrm{H\text{-}Ram}}(L)$ can be explained as follows: For the longer spans with fixed $G_{\mathrm{oo}} = 10$ dB, the H-Raman gain amplifies the weak signal power at the end of the spans; hence, less power per channel is available, leading to a lower four wave mixing (FWM) interaction among the channels and hence less NLI. However, with shorter spans, the signal power remains higher with less attenuation, and H-Raman with high $G_{\mathrm{oo}} = 10$ dB amplifies this strong signal power leading to stronger FWM interaction and NLI coefficients. In general, with longer spans, the NLI predictions of the GN model are better.

TABLE II
CALCULATED AND PREDICTED VALUES FOR $X_m^{\mathrm{H\text{-}Ram}}(L)$ FOR H-RAMAN

	FG = 50 GHz				FG = 12.5 GHz			
Span Length (km)	Calculated $X_m^{\mathrm{H\text{-}Ram}}(L)$	Standard Deviation	Predicted $X_m^{\mathrm{H\text{-}Ram}}(L)$	Error	Calculated $X_m^{\mathrm{H\text{-}Ram}}(L)$	Standard Deviation	Predicted $X_m^{\mathrm{H\text{-}Ram}}(L)$	Error
40	0.00103936	2.58079E − 06	0.00103948	1.23E − 07	0.00128603	2.2988E − 06	0.00128603	3.98415E − 09
50	0.00074133	1.89936E − 06	0.00074101	3.22E − 07	0.000914518	1.7001E − 06	0.00091407	4.386E − 07
60	0.00059683	1.50081E − 06	0.00059713	3.00E − 07	0.000736439	1.3373E − 06	0.00073682	3.84971E − 07
80	0.00049383	1.16785E − 06	0.00049361	2.18E − 07	0.000611332	1.0273E − 06	0.00061108	2.46065E − 07
100	0.00046822	1.07548E − 06	0.00046829	7.28E − 08	0.000580652	9.4081E − 07	0.00058081	1.62381E − 07
120	0.00046110	1.04945E − 06	0.00046103	6.96E − 08	0.00057211	9.1635E − 07	0.00057207	3.89802E − 08

TABLE III
COEFFICIENT VALUES FOR $X_m^{\text{H-Ram}}(L)$ PREDICTIONS

FG	a	b	c	d
50 GHz	0.01075	−0.07331	0.0004706	−0.0002005
12.5 GHz	0.01389	−0.07449	0.000585	−0.00022

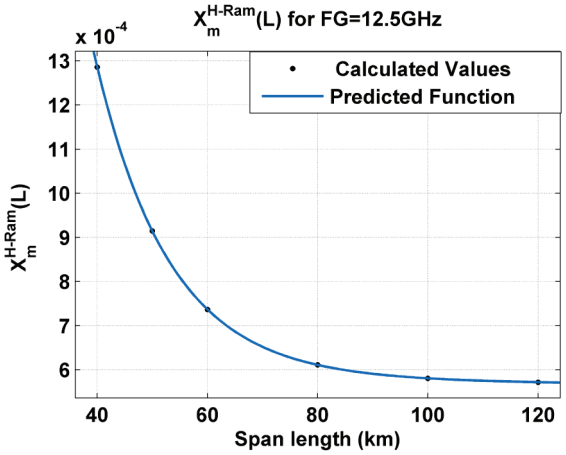

Fig. 2. Plots for $X_m^{\text{H-Ram}}(L)$ at FG = 12.5 GHz.

C. Effective Noise Figure for the H-Raman System

For the H-Raman case, we have a backward-pumped Raman system followed by an EDFA amplifier [11,12] with noise figure F_{EDFA}, as shown in Fig. 3:

$$N_{\text{eff}}^{\text{HRam}} = \left[2e^{-\alpha L} + \frac{2\alpha L_{\text{eff}}}{\text{In}G_{\text{oo}}}\left(1-\frac{1}{G_{\text{oo}}}\right) - \frac{1}{G_{\text{oo}}}\right] + \frac{F_{\text{EDFA}}-1}{G_{\text{oo}}}. \quad (12)$$

In Eq. (12) $N_{\text{eff}}^{\text{HRam}}$ gives an effective noise figure for a Raman EDFA hybrid amplifier, and the first term inside the square brackets models the effective noise figure of the Raman amplification part as an imaginary amplifier [12–14]. The above effective noise figure accounts for the ASE noise produced by an imaginary discrete amplifier, which captures noise from a distributive amplification system such as H-Raman [14,15].

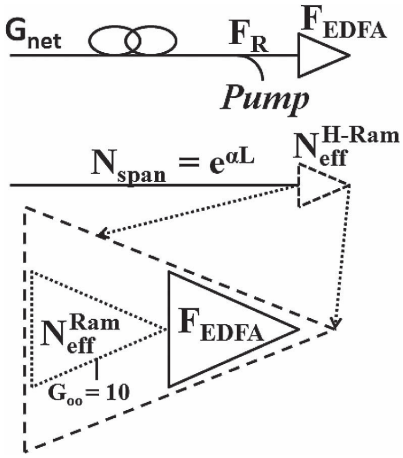

Fig. 3. Noise model for the H-Raman system for $G_{\text{oo}} = 10$ dB.

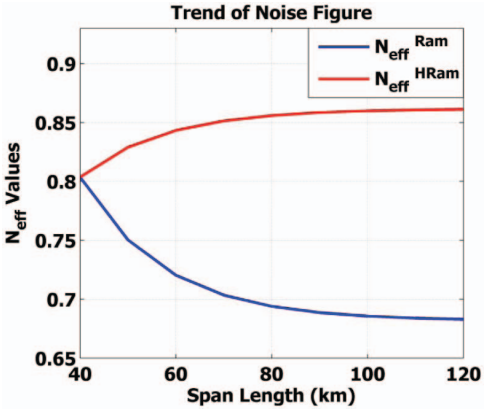

Fig. 4. N_{eff} plots for H-Raman and only Raman for $G_{oo} = 10$ dB.

The plot in Fig. 4 shows the effective noise figure, N_{eff}. For an only Raman system, the effective noise figure $N_{\text{eff}}^{\text{Ram}}$ will rise as we reduce the span length. In order to maintain G_{oo} of 10 dB, we need to increase the pump power for shorter span lengths, which will increase the noise and $N_{\text{eff}}^{\text{Ram}}$. Regarding the $N_{\text{eff}}^{\text{HRam}}$, the effective noise figure for H-Raman, for longer span lengths the EDFA will provide the majority of gain and hence will dominate the noise. However, as the span length decreases, the effect of the EDFA noise figure will diminish, and at 40 km span length, which amounts to 10 dB loss, only the Raman part is needed to compensate for the span loss. Therefore, the N_{eff} values of H-Raman and all Raman converge, as in Fig. 4. Most of the Raman systems, considering practical pump levels, have a G_{oo} range of 10–15 dB [12]. In this study, we choose the starting value of $G_{oo} = 10$ dB because it is a typical value [16] and also to have a fair comparison with EDFAs whose typical inter-span length ranges from 40 to 120 km [8]; using $G_{oo} = 10$ dB and launch power optimization, we can reach this minimum span length of 40 km while assuming $\alpha = 0.25$ dB/km.

D. Expression of Optimum Launch Power for H-Raman

In Fig. 5 N_i^{HRam} are the intermediate H-Raman amplifier's effective noise figures and each compensates exactly for their previous span loss. $N_{\text{last}}^{\text{HRam}}$ is the effective noise figure of the last amplifier, which not only compensates for the last span loss but also increases the signal power from $P_{\text{opt}}^{\text{new}}$ to P_r. For the last amplifier, the extra gain is provided by the EDFA part of the H-Raman amplifier.

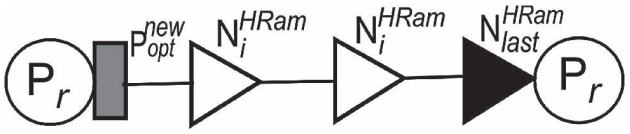

Fig. 5. H-Raman in-line amplifiers in new network scenario.

F^i_{EDFA} and $F^{\text{last}}_{\text{EDFA}}$ are the noise figures for the EDFAs in the intermediate and last H-Raman amplifier. For n_{sp} of 1.4, we can write

$$F^i_{\text{EDFA}} = \frac{2n_{\text{sp}}(G^i_{\text{EDFA}} - 1)}{G^i_{\text{EDFA}}} + \frac{1}{G^i_{\text{EDFA}}}, \tag{13}$$

where G^i_{EDFA}, $G^{\text{last}}_{\text{EDFA}}$ are gains of EDFA amplifiers in the intermediate and last H-Raman setup and G is equivalent to linear span loss:

$$G^{\text{last}}_{\text{EDFA}} = \frac{P_r}{P^{\text{new}}_{\text{opt}}} G^i_{\text{EDFA}} = \frac{P_r}{P^{\text{new}}_{\text{opt}}} \frac{G}{10}, \tag{14}$$

$$F^{\text{last}}_{\text{EDFA}} = F^i_{\text{EDFA}} + \frac{(2n_{\text{sp}} - 1)\left(1 - \frac{P^{\text{new}}_{\text{opt}}}{P_r}\right)}{G^i_{\text{EDFA}}}. \tag{15}$$

Using Eq. (14), the relation between $N^{\text{HRam}}_{\text{last}}$ and N^{HRam}_i is

$$N^{\text{HRam}}_{\text{last}} = N^{\text{HRam}}_i + \frac{(2n_{\text{sp}} - 1)\left(1 - \frac{P^{\text{new}}_{\text{opt}}}{P_r}\right)}{G}. \tag{16}$$

The total amplified spontaneous noise for a single optical link, ASE_0 (mW) is calculated from Eq. (17) where ASE_1 and ASE_2 can be calculated from N^{HRam}_i and $N^{\text{HRam}}_{\text{last}}$:

$$\text{ASE}_0 = \left[\frac{P_r}{P^{\text{new}}_{\text{opt}}}(N_S - 1)\text{ASE}_1 + \text{ASE}_2\right], \tag{17}$$

$$\text{ASE}_0 = \left(\frac{P_r}{P^{\text{new}}_{\text{opt}}}(N_s N^{\text{HRam}}_i G + 2n_{\text{sp}} - N_s)hvB_{\text{ref}} - 2.8hvB_{\text{ref}}\right). \tag{18}$$

Following the similar procedure in Eq. (7) of differentiating for $P^{\text{new}}_{\text{opt}}$ to find the maximum OSNR for a given link, using Eq. (18) we get

$$P^{\text{new}}_{\text{opt}} = \left[\frac{((N_s N^{\text{HRam}}_i G) + 2n_{\text{sp}} - N_s)hvB_{\text{ref}}}{2N_s X^{\text{H-Ram}}_m(L)}\right]^{1/3}. \tag{19}$$

Here, P_r is about 1.25 mW at MaxSpan = 120 km, but in further sections we use $P_r = 1.6$ mW for both EDFA and H-Raman to have a fair comparison. For all our calculations, we have assumed an undepleted pump with small signal assumption [14], where, even for small span lengths up to 40 km and 133 channels with FG = 12.5 GHz, the optimum signal power per channel is about 0.2 mW, which is significantly less than the signal power limit of about 1.2 mW per channel for only the Raman case with SSMF Raman gain efficiency, $CR = 0.35\ (\text{W}\cdot\text{km})^{-1}$ [17] to comply with the undepleted pump assumption.

III. Benefits of Improved ROADM OSNR Conditions

Having developed the understanding of the noise model, in this section we explore the benefits of improved OSNR conditions at ROADMs. The observations help service providers to understand that, if the line noise is dominant in their network lightpaths, improving ROADM OSNR might not yield sufficient capacity benefits.

TABLE IV
OSNR Threshold and Pcap Factor for Modulation Formats

Modulation	Capacity	Pcap	OSNR
PM-BPSK	100	5	9 dB
PM-QPSK	100	2	12 dB
PM-8QAM	150	1.5	16 dB
PM-16QAM	200	1	18.6 dB
PM-32QAM	250	0.5	21.6 dB
PM-64QAM	300	0	24.6 dB

Here the P_r value is increased from 1.6 to 5 mW, in order to have a worthwhile OSNR gain at the ROADMs to explicitly demonstrate the benefit of improved ROADM OSNR conditions. As mentioned earlier, increasing P_r also increases the ASE_0 and η_{NLI}, which has been considered in our study.

A potential capacity factor (Pcap) [7,14] indicates how many extra 100G demands a lightpath can carry, if it improves its OSNR to operate at the highest given modulation format, assumed to be PM-64QAM in this work. Table IV gives the Pcap factors for various modulation formats and indicative OSNR thresholds [18].

The capacity constraint factor in Eq. (20) gives a measure of how much the Pcap factor remains per lightpath. This gives a true indication of the network state in terms of capacity. This is shown in Fig. 6 for three lightpaths, where a CC factor of 2.33 highlights that, on average, network lightpaths need to increase their OSNR:

$$\text{CC Factor} = \frac{\text{Total Pcap of all Lightpaths}}{\text{No. of Lightpaths}}. \tag{20}$$

The results in Tables V and VI are averaged over 30 different traffic matrices of static 100G demands for each network topology scenario and P_r values of 1.6 and 5 mW for EDFA and H-Raman. Simulations are performed using shortest path routing. The network performance parameter used here is 10% blocking for new demands. The UK, Pan-EU, and US network topologies have been chosen for

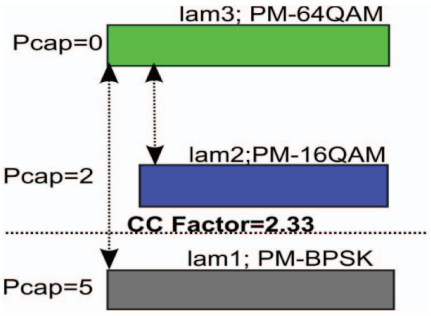

Fig. 6. Example of Pcap and CC factor for three lightpaths.

TABLE V
AVERAGE NUMBER OF ALLOCATED DEMANDS FOR FG = 50 GHz OF 30 MATRICES

MaxSpan	Allocated Demands (EDFA)						Allocated Demands (H-Raman)					
	50 km		60 km		120 km		50 km		60 km		120 km	
P_r (mW)	1.6 mW	5 mW	1.6 mW	5 mW	1.6 mW	5 mW	1.6 mW	5 mW	1.6 mW	5 mW	1.6 mW	5 mW
UK	1156.7	1169.2	1132.6	1155.6	868.8	880.9	1207.8	1243.7	1187.9	1243.7	1058.1	1097.6
Pan-EU	1066.5	1078.1	990.7	1012.4	540.3	540.3	1235.9	1259.1	1193.2	1204.5	724.5	731.1
USA	377.3	382.1	351.3	355.5	216.6	216.6	530.1	546.7	516.2	530.2	341.2	341.2

TABLE VI
AVERAGE NUMBER OF ALLOCATED DEMANDS FOR FG = 12.5 GHz OF 30 MATRICES

MaxSpan	Allocated Demands (EDFA)						Allocated Demands (H-Raman)					
	50 km		60 km		120 km		50 km		60 km		120 km	
P_r (mW)	1.6 mW	5 mW	1.6 mW	5 mW	1.6 mW	5 mW	1.6 mW	5 mW	1.6 mW	5 mW	1.6 mW	5 mW
UK	1639.8	1648.4	1597.7	1639.5	1174.8	1196.1	1689.1	1749.4	1671.2	1737.7	1486.2	1523.2
Pan-EU	1424	1441	1302.1	1316	671.8	672.1	1649.9	1695.4	1603.8	1625.8	968.4	985.4
USA	476.33	476.3	448.1	452.6	257.3	257.3	691.5	699.63	663.8	676.5	443.2	450.43

simulation based upon their geographical area, increased link lengths, and reduced node density, as shown in Fig. 7.

As can be seen in Tables V and VI, with reducing MaxSpan, the allocated demand count increases in the case of EDFA and H-Raman, showing that, by optimizing the signal power, we are able to counter the effects of NLI. In the case of H-Raman, the traffic demand count is higher in FG = 50 and 12.5 GHz depicting the superior noise performance for H-Raman compared with EDFA.

In Fig. 8 it is evident that there is a progressive reduction in high benefit histograms as we move from small UK to large US networks, by increasing P_r from 1.6 to 5 mW.

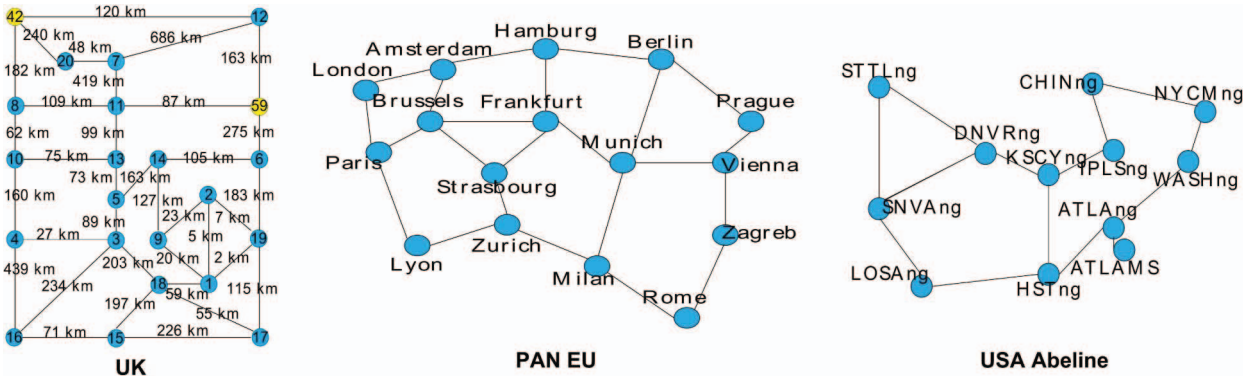

Fig. 7. Network topologies.

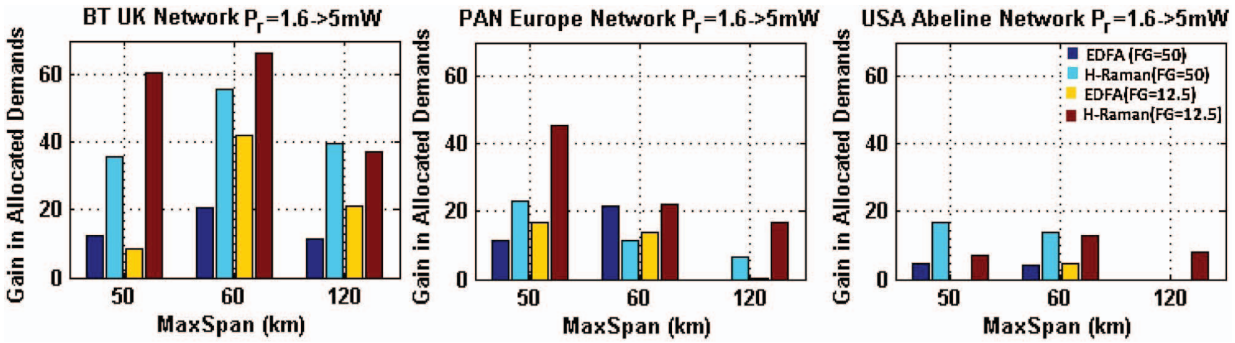

Fig. 8. Trend of increasing P_r with different network topologies.

Two characteristics in the network influence this behavior. First, the UK has small link lengths compared with the US and Pan-EU networks; therefore, the line noise in the UK network is lower. Second, the UK network has a high density of nodes, with 2.2 hops per lightpath compared with 1.7 and 1.2 hops per lightpath in the Pan-EU and US networks. This further increases the impact of improved OSNR conditions at network nodes on a lightpath OSNR.

It also can be seen that, at MaxSpan = 120 km, the increase in demand count is considerably lower than when MaxSpan = 60 or 50 km for the Pan-EU and US. In Eq. (3) it can be seen that, if the line noise heavily dominates the lightpath OSNR, improving the ROADM OSNR might not bring much improvement in the overall lightpath OSNR, and this is precisely why at MaxSpan = 120 km we do not see any improvement with EDFAs and only a small improvement with H-Raman for the larger networks. Further, as the span lengths decrease to 60 or 50 km, the line noise component reduces and becomes comparable with the ROADM noise for the majority of the lightpaths; therefore, improved ROADM OSNR is generally beneficial either with EDFA or H-Raman with H-Raman providing maximum gains in most of the cases. Also, at smaller spans the scope for improvement of lightpath capacity is less, e.g., in the UK at MaxSpan = 50 km, most of the lightpaths are operating at PM-64QAM and with a much smaller number at PM-32QAM, and so increasing P_r causes very few lightpaths to make the transition to PM-64QAM; thus, overall slightly less improvement is found. However, the difference in capacity gains between large span regions of 120 km and smaller span regions of 60–50 km can be seen clearly in Fig. 8.

Therefore, from these results, it is seen that networks with dominant line noise and less node density will least benefit from better ROADM architectures. These networks need higher G_{oo}-based Raman amplifiers or superior optical equipment, which can significantly reduce line noise. In smaller geographies or networks, such as in the UK where line noise is already small and with high node density, superior ROADMs can be used to enable higher capacities.

IV. Offline Strategy for Amplifier Addition

The above model can be used where, through progressive targeted addition of line amplifiers, we can improve the OSNR conditions of existing lightpaths and hence increase the overall network capacity.

Using the Pcap concept, we can calculate $P\text{cap}f_i$ for the ith fiber link and $P\text{cap}f_n$ for network Pcap. Here n_{bi}, n_{qpi}, n_{q8i}, n_{q16i}, and n_{q32i} are the number of lightpaths using PM-BPSK, PM-QPSK, PM-8QAM, PM-16QAM, and PM-32QAM, respectively, that are passing over the ith fiber, and n_{bn}, n_{qpn}, n_{q8n}, n_{q16n}, and n_{q32n} are the total number of lightpaths in each modulation format in a particular network state:

$$P\text{cap}f_i = 5n_{bi} + 2n_{qpi} + 1.5n_{q8i} + 1n_{q16i} + 0.5n_{q32i}, \quad (21)$$

$$P\text{cap}f_n = 5n_{bn} + 2n_{qpn} + 1.5n_{q8n} + 1n_{q16n} + 0.5n_{q32n}. \quad (22)$$

A. Offline Amplifier Addition Strategy

1. We begin with a baseline network with MaxSpan = 120 km and $P_r = 1.6$ mW with K extra units of amplifiers available to be added in subsequent steps.
2. For a given traffic matrix, lightpaths are allocated with this configuration until 10% blocking of demands occurs. Further, original network Pcap, $P\text{cap}f_n^{\text{ori}}$ and a normalized list of fiber links Pcap, $P\text{cap}f_i$ is calculated.
3. For each fiber link we calculate by how much the original $P\text{cap}f_n^{\text{ori}}$ reduces if an amplifier is added to the fiber link. This reduction is recorded as $\Delta P\text{cap}f_i^{\text{net}}$.
4. While executing step 3, we also keep a record of link OSNR gain for an amplifier addition to an ith fiber link, O_{gain}^i, and normalize the O_{gain}^i values.
5. We calculate the fitness cost function for a ith fiber link:

$$\text{Fitness}_i = \Delta P\text{cap}f_i^{\text{net}} + P\text{cap}f_i \times O_{\text{gain}}^i. \quad (23)$$

Using the above cost function, we generate fitness values for fiber links and choose a fiber link for an amplifier addition based on highest fitness value. Once an amplifier is placed, the network configuration is updated, and the procedure from step 2 onward is repeated while keeping the same traffic matrix, to monitor the benefits of added amplifiers offline. These steps are repeated until either all the K amplifiers are used or all fiber links reach the minimum span length criterion. Beyond this, we increase P_r to 5 mW. The fitness function helps us to choose a fiber link where adding an amplifier brings the maximum reduction in Pcap of the overall network, allowing network lightpaths to maximally increase network capacity. We want the fitness function to be dominated by this high gradient change. The role of the normalized product is to help us choose a fiber link in cases when there is no change in Pcap of the network for any fiber link.

B. Simulation Results and Discussion

To demonstrate the effectiveness of this strategy, simulations are performed on the three networks for both FG = 50 and 12.5 GHz at the OSNR limit for both EDFA and H-Raman configurations. A uniformly distributed random traffic matrix is generated, and while maintaining the same matrix, we carry out the amplifier addition process. The traffic matrix is made up of static 100G demands, and each resultant lightpath is based on a single shortest path computation.

As we have $G_{oo} = 10$ dB, we keep the minimum span length of 40 km. Because we reach the minimum span length criterion for the UK network after adding 45 amplifiers ($K = 45$), we maintain this value for other network simulations for a fair comparison. Demands allocated for each modulation format are recorded until 10% blocking is reached. The results are averaged over 10 different randomly generated matrices.

As can be seen from the UK network results in Fig. 9, demands readily migrate to PM-64QAM due to the

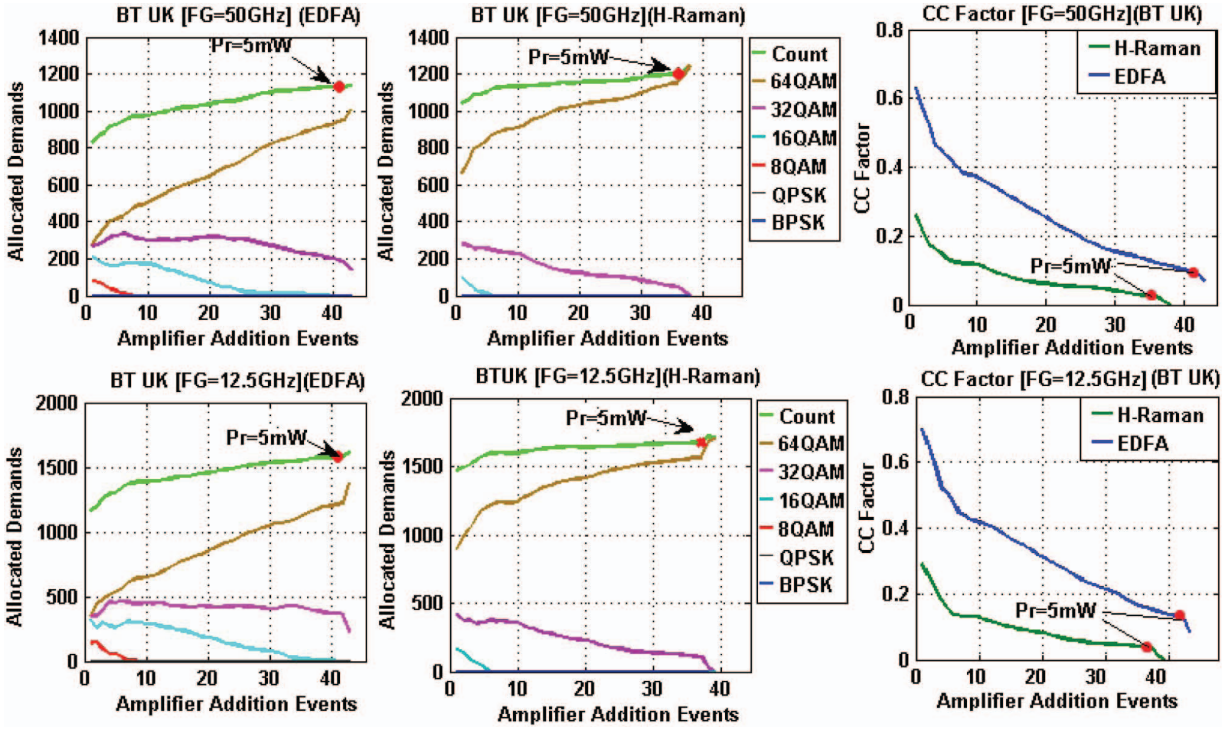

Fig. 9. Performance of offline strategy results for the UK network.

radically improving OSNR of this small network. This leads to rapid reduction in the overall Pcap of the network and low CC factor values. Further, the strategy uses 38 amplifiers in the case of the H-Raman system to reach CC factor = 0 compared with 45 units of EDFA, thereby reducing the wastage of equipment as the network has achieved its ideal state of CC = 0. Starting with MaxSpan of 120 km, we increase the network capacity for both the EDFA and H-Raman cases, where 7.5% extra capacity is achieved through the use of H-Raman. This small benefit is due to smaller link lengths in the network where EDFA and H-Raman both perform well. However, it should be noted that, by using H-Raman, we achieve the ideal network condition with CC factor = 0 and all lightpaths operating at the PM-64QAM. Therefore, for H-Raman, up to G_{oo} = 10 dB is good enough for the UK network.

The results of the UK network also are in consonance with the improved ROADM OSNR results in Section III, where increasing the P_r value from 1.6 to > 5 mW results in increased tendency to use PM-32QAM and PM-64QAM. This is also manifested in the CC factor curves with tangible drops in CC factors, seen as P_r is increased. This shows that the UK network lightpaths will be much more responsive to better ROADM equipment.

As the Pan-EU and US networks are geographically bigger with large link lengths, as shown in Table VII, the inherent OSNR of these networks is lower compared with the UK network. Also line noise is more dominant for these networks at higher span lengths. Because of this, EDFA in-line amplifiers are the main bottleneck preventing ideal CC factor values and high capacity. Larger networks will benefit less from EONs with in-line EDFAs, resulting in high CC factor values of 3.5 and 4.5 in the Pan-EU and USA network, respectively. As shown in Figs. 10 and 11, count curves are linear for Pan-EU and nearly flat for US with in-line EDFAs. H-Raman alleviates this issue for larger networks with capacity increase of 35% and 94.9% increase for Pan-EU and US networks compared with EDFA at the end of the procedure. The CC factor also reduces to 0.8 and 1.5 for Pan-EU and USA networks with H-Raman, due its superior noise performance. However, compared with the UK network, we are still far away from the ideal condition of $CC = 0$, and considering that already we are using a high G_{oo} = 10 dB, efforts to design improved equipment with lower loss need to be the focus area of investment for larger networks.

Improving ROADM OSNR conditions in such a large network brings less tangible benefits in terms of capacity in Pan-EU and almost no benefits in the US network due to the longer link lengths, which results in highly dominant line noise and smaller node density. This reduces the benefits of improved ROADM OSNR conditions. Little improvement is seen when using H-Raman.

TABLE VII
NETWORK NODES AND LINK DETAILS

Network	No. of Nodes	Average Link Length
UK	22	150 km
Pan-EU	16	490 km
USA Abeline	12	900 km

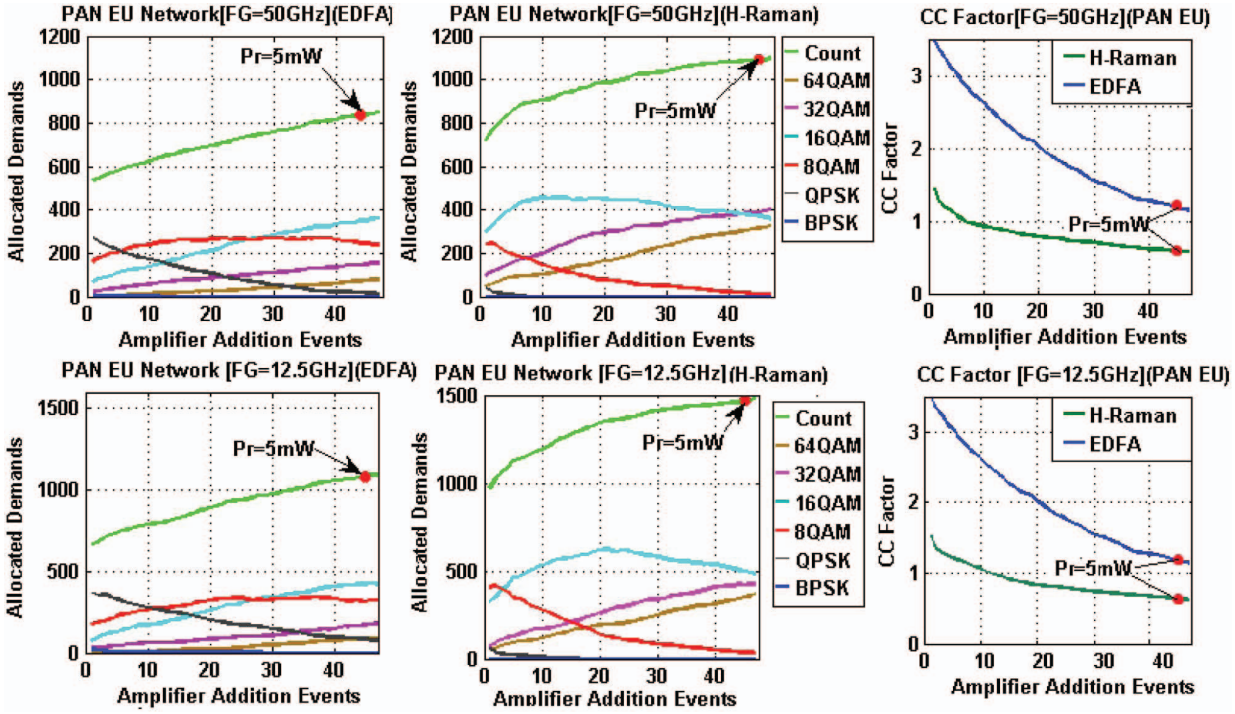

Fig. 10. Performance of offline strategy results for the Pan-European network.

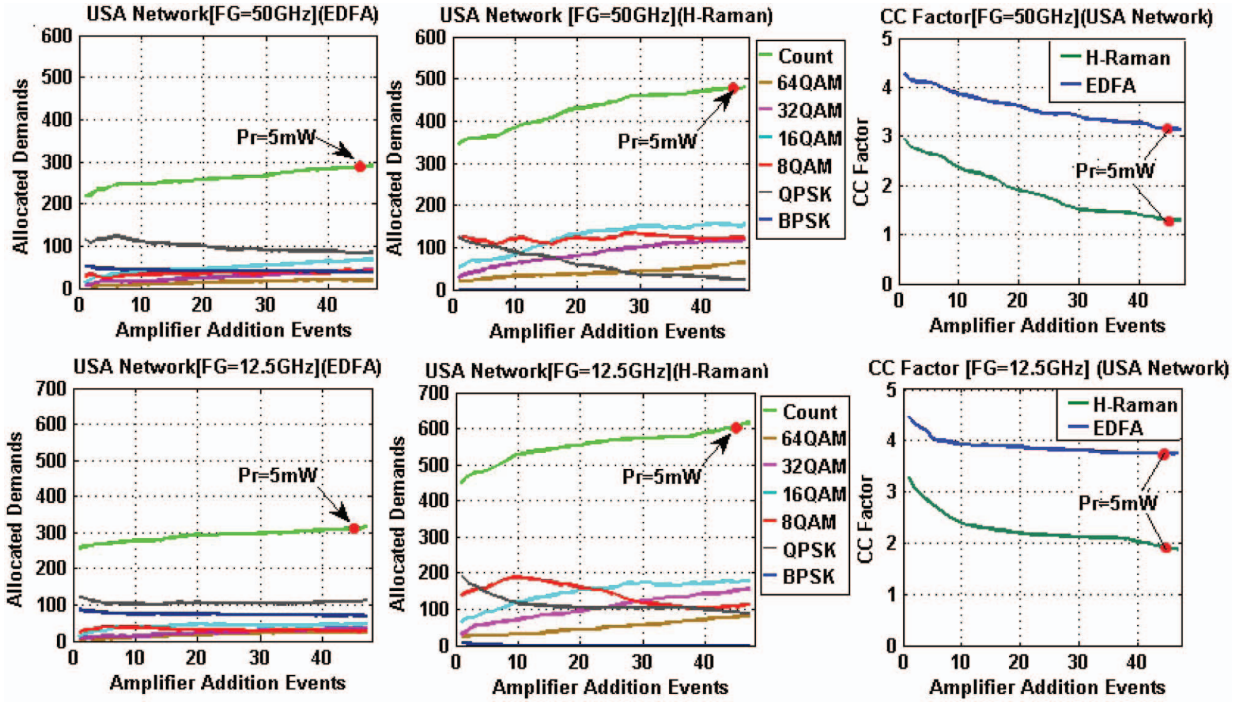

Fig. 11. Performance of offline strategy results for the US network.

V. Conclusion

Throughout the first few sections, a simple model, which segregates the noise and consequently the OSNR contribution by in-line amplifiers and ROADMs to the OSNR of a network lightpath, has been shown.

Further, it has been shown that higher benefits in network capacity can be achieved when improvement of

ROADM OSNR conditions is complemented by reduction of dominant line noise in the network lightpaths. This makes the lightpaths respond more toward improved ROADM OSNR conditions. Generally, having smaller span lengths between the in-line amplifiers help to reduce the dominant effect of line noise; hence, it is likely to give better capacity benefits while improving ROADM OSNR conditions.

It has been shown that the UK network is much more responsive to increased values of P_r compared with the Pan-EU and US networks owing to higher node density and smaller link lengths with less line noise. At $P_r =$ 5 mW and in-line H-Raman amplifiers, the CC factor for the UK network falls to 0, whereas the CC factor in the Pan-EU and US networks is still comparatively high. Therefore, developing better equipment, which can reduce the CC factor for larger networks, is required. Finally, an offline strategy method has been suggested, which effectively captures the heterogeneity of different modulation formats as per the EON paradigm and presents a strong knowledge base to make important decisions about the quantity and quality of in-line amplifiers to benefit from high-capacity EON lightpaths. The major advantage of the CC factors and offline strategy is that they are compatible with future use of modulation formats beyond PM-64QAM.

Appendix A: Derivation of the $X_m^{\text{H-Ram}}(L)$ Expression for H-Raman

The PSD of the nonlinear interference for a single-span NLI, $G_{\text{NLI,SS}}$ is given by [6,19,20]

$$G_{\text{NLI,SS}} = \frac{16}{27}\gamma^2 L_{\text{eff}}^2 \int_{-\infty}^{\infty}\int_{-\infty}^{\infty} G(f_1)G(f_2)G(f_1+f_2-f) \times \rho(f_1,f_2,f_3)\mathrm{d}f_1\mathrm{d}f_2. \tag{A1}$$

In the above expression the signal power spectral densities, $G(f)$, for FG = 12.5 GHz and FG = 50 GHz are given by Eqs. (A2) and (A3). Channels are assumed to be Nyquist-shaped:

$$G(f) = \frac{P_0}{R}\sum_{i=-66}^{66}\mathrm{rect}\left(\frac{f-i\Delta f}{R}\right) = P_0 g(f). \tag{A2}$$

$$G(f) = \frac{P_0}{R}\sum_{i=-49}^{50}\mathrm{rect}\left(\frac{f-i\Delta f}{R}\right) = P_0 g(f). \tag{A3}$$

Here P_0 is the launch power of each channel and R is the symbol rate of 27.75 GBaud with Δf being channel spacing of 37.5 GHz in FG = 12.5 GHz system and 50 GHz in FG = 50 GHz system.

The receiving matched filter is given by

$$H(f) = \mathrm{rect}\left(\frac{f}{R}\right). \tag{A4}$$

Now, because we are concerned with traditional OSNR over B_{ref} of 12.5 GHz, we need to accumulate the PSD expression over the received matched filter and then convert it into the reference bandwidth of B_{ref}. Defining $g(f) = G(f)/P_0$, the following expression in Eqs. (A5) and (A6) gives NLI and $X_m^{\text{H-Ram}}(L)$ over a single span:

$$\eta_{\text{NLI}}^{1\text{ span}} = \frac{B_{\text{ref}}}{R}\frac{16}{27}\gamma^2 P_0^3 \int_{-\infty}^{\infty}\int_{-\infty}^{\infty}\int_{-\infty}^{\infty}[g(f_1)g(f_2)g(f_1+f_2-f) \times H(f)L_{\text{eff}}^2\rho(f_1,f_2,f)\mathrm{d}f_1\mathrm{d}f_2\mathrm{d}f], \tag{A5}$$

$$X_m^{\text{H-Ram}}(L) = \frac{B_{\text{ref}}}{R}\frac{16}{27}\gamma^2 \int_{-\infty}^{\infty}\int_{-\infty}^{\infty}\int_{-\infty}^{\infty}\Big[g(f_1)g(f_2)g(f_1+f_2-f) \times H(f)L_{\text{eff}}^2\rho(f_1,f_2,f)\mathrm{d}f_1\mathrm{d}f_2\mathrm{d}f\Big]. \tag{A6}$$

For the H-Raman case, the term $L_{\text{eff}}^2\rho(f_1,f_2,f)$ accounting for four wave mixing (FWM) efficiency is given by [6,19]

$$L_{\text{eff}}^2.\rho(f_1,f_2,f) = \left| \begin{array}{c} \frac{e^{-\frac{C_R P_{P0}}{\alpha_p}}}{\alpha_P}\left(-\frac{C_R P_{P0}}{\alpha_P}\right)^{\left[\frac{\alpha}{\alpha_p}-\frac{j4\pi^2\beta_2(f_1-f)(f_2-f)}{\alpha_p}\right]} \\ \left[\Gamma\left(\left\{\frac{j4\pi^2\beta_2(f_1-f)(f_2-f)}{\alpha_p}-\frac{\alpha}{\alpha_p}\right\},-\frac{C_R P_{P0}}{\alpha_P}\right)\right. \\ \left.-\Gamma\left(\left\{\frac{j4\pi^2\beta_2(f_1-f)(f_2-f)}{\alpha_p}-\frac{\alpha}{\alpha_p}\right\},-\frac{C_R P_{P0}}{\alpha_p}e^{\alpha_p L}\right)\right] \end{array} \right|^2, \tag{A7}$$

where C_R, P_{P0} are Raman gain efficiency and the pump power remaining at the beginning of the fiber, and we assume negligible pump depletion, and Γ is the upper complete gamma function. These are related to the on–off Raman gain, G_{oo} [20] where L is the span length:

$$G_{oo} = e^{\left\{\frac{C_R P_{P0}\,1-e^{-\alpha_p L}}{\alpha_p\quad e^{-\alpha_p L}}\right\}}. \tag{A8}$$

Thus, we can find the combination of C_R, P_{P0} in Eq. (A8), which can be written as

$$C_R P_{P0} = \log_e(G_{oo})\frac{\alpha_p e^{-\alpha_p L}}{1-e^{-\alpha_p L}}. \tag{A9}$$

For the backward pumping case, we further need Eq. (A10) where P_{P0} is related to P_{pump}, which is the pump power injected at the end of the fiber given by [20]

$$P_{P0} = P_{\text{pump}}e^{-\alpha_p L}. \tag{A10}$$

Therefore, substitute Eqs. (A2)–(A4), (A7), (A9), and (A10) in Eq. (A6), to calculate the $X_m^{\text{H-Ram}}(L)$ values. The integration of Eq. (A6) is done by the Monte Carlo simulation method, which gives us values with some degree of uncertainty.

Appendix B: Derivation of Effective Noise Figure for H-Raman

The total noise figure of a Raman system for a B_{ref} bandwidth and net optical gain G_{net} is given by [14]

$$F_R = \frac{2P_A^+}{G_{\text{net}}h\nu B_{\text{ref}}} + \frac{1}{G_{\text{net}}}, \tag{B1}$$

where P_A^+ is the spontaneous noise power for a single polarization:

$$P_A^+ = G_{\text{net}} h\nu n_{\text{eq}}^- B_{\text{ref}}. \tag{B2}$$

In Eq. (B1), n_{eq}^- is the spontaneous photon number [13] for the backward pump case, which is given by

$$n_{\text{eq}}^- = 1 - \frac{1}{G_{\text{net}}} + \frac{\alpha}{a_0}\left(e^{\alpha L} - \frac{1}{G_{\text{net}}}\right). \tag{B3}$$

In [11,12] equating G_{net} we find that

$$\ln G_{oo} = a_0 L_{\text{eff}}, \tag{B4}$$

$$a_0 = \gamma_0 n_p^0. \tag{B5}$$

Here γ_0, n_p^0 are the Raman gain factor and input photon number. L_{eff} is the effective interaction length as in [11]. Using the above equations with $G_{\text{net}} = e^{-\alpha L} G_{oo}$ [14] and substituting into Eq. (B1), we get the total noise figure of the backward-pumped Raman amplification system:

$$F_R = e^{\alpha L}\left[2e^{-\alpha L} + \frac{2\alpha L_{\text{eff}}}{\ln G_{oo}}\left(1 - \frac{1}{G_{oo}}\right) - \frac{1}{G_{oo}}\right]. \tag{B6}$$

By the Friis formula, the total noise figure of the setup is calculated by

$$F_T = F_R + \frac{F_{\text{EDFA}} - 1}{G_{\text{net}}} = e^{\alpha L} N_{\text{eff}}^{\text{HRam}}. \tag{B7}$$

Substituting Eq. (B7) with $G_{\text{net}} = e^{-\alpha L} G_{oo}$, in Eq. (B7), we get

$$N_{\text{eff}}^{\text{HRam}} = \left[2e^{-\alpha L} + \frac{2\alpha L_{\text{eff}}}{\ln G_{oo}}\left(1 - \frac{1}{G_{oo}}\right) - \frac{1}{G_{oo}}\right] + \frac{F_{\text{EDFA}} - 1}{G_{oo}}. \tag{B8}$$

Acknowledgment

We would like to acknowledge Bharti School of Telecommunication Technology and Management, IIT Delhi, for providing the research facilities and support to conduct this work. Further, we would like to sincerely thank the INSIGHT project at UCL for facilitating this technical discussion.

References

[1] M. Jinno, H. Takara, B. Kozicki, Y. Tsukishima, Y. Sone, and S. Matsuoka, "Spectrum-efficient and scalable elastic optical path network: Architecture, benefits, and enabling technologies," *IEEE Commun. Mag.*, vol. 47, no. 11, pp. 66–73, Nov. 2009.

[2] O. Gerstel, M. Jinno, A. Lord, and S. J. B. Yoo, "Elastic optical networking: A new dawn for the optical layer?" *IEEE Commun. Mag.*, vol. 50, no. 2, pp. s12–s20, Feb. 2012.

[3] L. Velasco, P. Wright, A. Lord, and G. Junyent, "Saving CAPEX by extending flexgrid-based core optical networks toward the edges," *J. Opt. Commun. Netw.*, vol. 5, pp. A171–A183, Aug. 2013.

[4] O. Pedrola, A. Castro, L. Velasco, M. Ruiz, J. P. Fernandez-Palacios, and D. Careglio, "CAPEX study for multilayer IP/MPLS-over-flexgrid optical network," *J. Opt. Commun. Netw.*, vol. 4, pp. 630–650, Mar. 2012.

[5] P. Poggiolini, G. Bosco, A. Carena, R. Cigliutti, V. Curri, F. Forghieri, R. Pastorelli, and S. Piciaccia, "The LOGON strategy for low-complexity control plane implementation in new-generation flexible networks," in *Optical Fiber Communication Conf. and Expo. and the Nat. Fiber Optic Engineers Conf. (OFC/NFOEC)*, Anaheim, California, 2013, paper OW1H.3.

[6] P. Poggiolini, G. Bosco, A. Carena, V. Curri, Y. Jiang, and F. Forghieri, "The GN-model of fiber non-linear propagation and its application," *J. Lightwave Technol.*, vol. 32, no. 4, pp. 694–721, Feb. 2014.

[7] A. Mitra, D. Ives, A. Lord, S. Kar, and P. Wright, "Non-linear modeling in flexgrid network and its application in offline network equipment strategy," in *Optical Networks Design and Modelling Conf.*, Pisa, Italy, 2015, paper Tu4.20.

[8] R. J. Essiambre, G. Kramer, P. J. Winzer, G. J. Foschini, and B. Goebel, "Capacity limits of optical fiber networks," *J. Lightwave Technol.*, vol. 28, pp. 662–701, 2010.

[9] A. Ahmad, A. Bianco, H. Chouman, V. Curri, G. Marchetto, and S. Tahir, "A transmission aware network design for fixed and flexible grid optical networks," in *Int. Conf. on Transparent Optical Networks*, Budapest, 2015, pp. 1–4.

[10] A. Ahmad, A. Bianco, H. Chouman, V. Curri, G. Marchetto, and S. Tahir, "On the importance of detailed transmission layer modelling in optical network design," in *Fotonica AEIT Italian Conf. on Photonics Technologies*, Turin, 2015, pp. 1–4.

[11] V. Curri, A. Carena, P. Poggiolini, G. Bosco, and F. Forghieri, "Extension and validation of the GN model for non-linear interference to uncompensated links using Raman amplification," *Opt. Express*, vol. 21, pp. 3308–3317, 2013.

[12] M. N. Islam, *Raman Amplifiers for Telecommunications 2* (Springer Series in Optical Sciences, Vol. 90/2). Springer, 2004, pp. 413–445.

[13] E. Desurviere, *Erbium-Doped Fiber Amplifiers: Principles and Application*, 1st ed. Wiley Series in Telecommunications and Signal Processing. Wiley, 1994.

[14] J. Bromage, "Raman amplification for fiber communications systems," *J. Lightwave Technol.*, vol. 22, pp. 79–93, 2004.

[15] A. Mitra, A. Lord, S. Kar, P. Wrigth, and S. Debruslais, "Upgrading to low loss ROADMs and additional line amplifiers for increased capacity in EDFA and Raman flexgrid networks," in *European Conf. on Optical Communication (ECOC)*, Cannes, France, 2014, paper P.6.13.

[16] K. Porsezian and V. V. Kriakose, *Optical Solitons Theoretical and Experimental Challenges*. Springer, 2002.

[17] S. Namiki and Y. Emori, "Ultrabroad-band Raman amplifiers pumped and gain-equalized by wavelength-division-multiplexed high-power laser diodes," *IEEE J. Sel. Top. Quantum Electron.*, vol. 7, pp. 3–16, 2001.

[18] A. Lord, P. Wright, and A. Mitra, "Core networks in flexgrid era," *J. Lightwave Technol.*, vol. 33, pp. 1126–1135, 2015.

[19] D. Ives, P. Baywel, and S. J. Savory, "Adapting transmitter power and modulation format to improve optical network performance utilizing the Gaussian noise model of nonlinear impairments," *J. Lightwave Technol.*, vol. 32, pp. 4087–4096, 2014.

[20] P. Poggiolini, "The GN-model of non-linear propagation in uncompensated coherent optical systems," *J. Lightwave Technol.*, vol. 30, no. 24, pp. 3857–3879, 2012.